WIRELESS COMMUNICATIONS AND MOBILE COMPUTING
Wirel. Commun. Mob. Comput. (2016)
Published online in Wiley Online Library (wileyonlinelibrary.com). DOI: 10.1002/wcm.2701

RESEARCH ARTICLE

Selected mapping technique for reducing PAPR of single-carrier signals

Amnart Boonkajay* and Fumiyuki Adachi

Research Organization of Electrical Communication, Tohoku University, 2-1-1 Katahira, Aoba-ku, Sendai-shi, Miyagi, 980-8577 Japan

ABSTRACT

Single-carrier transmission with frequency-domain equalization (SC-FDE) is widely known as a promising transmission technique providing low error probability with low peak-to-average power ratio (PAPR) of transmit signal. However, the low-PAPR property of SC-FDE cannot be maintained if multi-level data modulation is introduced. The low-PAPR property of SC-FDE can be maintained by applying transmit filtering with roll-off factor at the expense of spectrum efficiency. In this paper, we propose two types of selected mapping (SLM) to reduce the PAPR of SC-FDE transmit signal. The first SLM technique is conducted in the frequency domain, where the phase rotation is applied to subcarriers similar to the SLM technique for orthogonal frequency division multiplexing transmission. The second SLM technique is conducted in the time domain, where the phase rotation is applied directly to data-modulated symbol sequence. Computer simulation confirms that both SLM techniques are able to reduce the PAPR of SC-FDE signal without significant degradation of bit-error rate performance and spectrum efficiency. Copyright © 2016 John Wiley & Sons, Ltd.

KEYWORDS

single-carrier (SC) transmission; selected mapping (SLM); frequency-domain equalization (FDE); peak-to-average power ratio (PAPR)

***Correspondence**

Amnart Boonkajay, Research Organization of Electrical Communication, Tohoku University, 2-1-1 Katahira, Aoba-ku, Sendai-shi, Miyagi, 980-8577 Japan.

E-mail: amnart@riec.tohoku.ac.jp

1. INTRODUCTION

Distributed antenna network [1], which achieves high spectrum efficiency (SE) and energy efficiency, is considered as a promising network architecture for the fifth-generation system. However, broadband wireless channel is characterized as a frequency-selective fading channel, in which inter-symbol interference significantly degrades the bit-error rate (BER) performance [2]. Orthogonal frequency division multiplexing (OFDM) [3] is a robust multi-carrier transmission technique, but its high peak-to-average power ratio (PAPR) of transmit signal is the main drawback. On the other hand, single-carrier transmission with frequency-domain equalization (SC-FDE) [4] is attractive for uplink communication because of its lower PAPR, while the use of FDE can effectively suppress the impact of inter-symbol interference.

Peak-to-average power ratio of SC signal becomes higher as higher level modulation is used. PAPR increases by 1 dB in SC-FDE when the modulation level is changed from 4 quadrature amplitude modulation (QAM) to 16 QAM [5]. This fact indicates the necessity of PAPR reduction technique even for SC transmission. Even though distributed antenna network can reduce the transmit power because of shorter range of transmission, PAPR reduction remains a significant issue in fifth-generation in order to further reduce the power consumption of linear power amplifier at the mobile terminal. We are also aiming at achieving very low-PAPR transmission (for example, 3 dB lower than the conventional SC-FDE) in uplink transmission in order to further improve the energy efficiency of user equipment. In general, PAPR of SC signal can be reduced by applying pulse shaping. Square-root raised-cosine (SRRC) pulse with roll-off factor of 0.5 can achieve 2 dB reduction of transmit PAPR in 16 QAM modulation [6], but the pulse with roll-off factor of 0.5 requires 1.5 times of transmission bandwidth and consequently degrades SE. Many transmit filtering techniques providing lower PAPR than SRRC pulse have been proposed as the techniques [7,8], but the PAPR reduction is obvious only when high roll-off factor is used. A transmit filtering based on minimum variance of instantaneous transmit power criterion can reduce the PAPR without SE degradation [9], but the PAPR reduction is marginal.

The existing PAPR reduction techniques for SC-FDE [7–9] are spectrum inefficient as discussed previously. This motivated us to develop a spectrum-efficient PAPR reduction technique for filtered SC signals. A simple approach is to study the PAPR reduction techniques for OFDM transmission. Many PAPR reduction techniques were extensively studied for OFDM transmission such as clipping [10] and coding [11]. However, these techniques still have drawbacks: clipping intentionally generates waveform distortion, and coding requires redundant bits. Among various PAPR reduction techniques, selected mapping (SLM) [12,13] is very attractive because it is a small-overhead, distortionless PAPR reduction technique with simple implementation by applying phase rotation to the subcarriers. It is shown in [12,13] that the SLM can effectively reduce the PAPR of OFDM signal with moderate computational complexity, and its PAPR-complexity tradeoff is much better than partial transmit sequence technique [14]. However, the SLM technique has been extensively studied only for OFDM signal.

In this paper, we introduce two approaches for implementing SLM in SC-FDE transmission and propose two SLM techniques corresponding to those implementation approaches for reducing the PAPR of SC-FDE signal. The first SLM technique is implemented by utilizing the fact that SC-FDE signal can be generated in frequency domain, that is, by inserting discrete Fourier transform (DFT) into conventional OFDM transmitter as a linear precoder [15]. This technique is called frequency-domain SLM (FD-SLM). The frequency components obtained by DFT are multiplied with a selected phase rotation pattern before performing inverse DFT (IDFT). The phase rotation pattern that provides the minimum PAPR is selected. The BER performance is kept intact; however, the transmission of so-called side information is necessary. On the other hand, the second SLM technique is implemented by utilizing the fact that the peak power of SC-FDE signals depends on an arrangement of data symbols in a transmission block [16]. In the second SLM technique, the phase rotation pattern is directly multiplied to data-modulated sequence block in time domain, in order to eliminate the symbol arrangement that causes high peak power. This technique is called the time-domain SLM (TD-SLM). The resultant time-domain transmit block candidates after multiplying each phase rotation pattern are pulse shaped by Nyquist pulse (which is equivalent to a process of applying a band-limited filtering in frequency domain), and then the best phase rotation pattern that provides the minimum PAPR is selected.

The novelty and contribution of this paper can be summarized as follows:

- A problem of high-PAPR signal in SC-FDE due to higher level modulation and then, the requirement of spectrum-efficient PAPR reduction technique for SC-FDE are discussed.
- To reduce the PAPR without significant SE degradation, two PAPR reduction techniques based on SLM for SC-FDE are proposed. This is our new contribution in this paper. The multiplication of selected phase rotation pattern can be carried out either in frequency domain or time domain. We also would like to mention that the phase rotation used in conventional SLM [12,13] for OFDM signal is available only in frequency domain.
- Performance evaluations of SC-FDE using the proposed SLM techniques are performed by computer simulation in aspects of PAPR, BER, throughput and computational complexity and are compared with that of the conventional SC-FDE (DFT-precoded SC-FDE) and SRRC-filtered SC-FDE. The evaluation results show that the proposed SLM techniques can reduce the PAPR of SC-FDE signals without significant degradation on BER and throughput performances. The TD-SLM provides lower PAPR than FD-SLM if the same number of phase rotation patterns is used. The analysis on PAPR reduction effects of both FD-SLM and TD-SLM is also provided in order to clarify why the TD-SLM gives lower PAPR than FD-SLM. Note that the SLM requires moderate computational complexity, and the study of complexity reduction is left as our future works because the problems of PAPR and spectrum efficiency are considered as higher priority than computational complexity in this paper.

The remaining of this paper is organized as follows. FD-SLM algorithm and its application in multi-level modulated SC-FDE are explained in Section 2. TD-SLM algorithm and its application in SC-FDE are described in Section 3. Section 4 shows the performance evaluations. Finally, Section 5 concludes the paper.

2. SC-FDE USING FD-SLM

An explanation of FD-SLM algorithm, together with its implementation in conventional SC-FDE block transmission, is provided in this section. Transmitted and received signal blocks are represented as column vectors, where the signal processing in each stage is represented by matrix throughout this paper.

2.1. FD-SLM algorithm

Selected mapping [12,13] has been introduced as a frequency-domain-based distortionless PAPR reduction technique with small overhead. In this paper, an FD-SLM is implemented to SC-FDE transmission, where the phase rotation is applied to the frequency-domain SC signal after DFT and prior to IDFT. The FD-SLM algorithm and its signal processing are simply illustrated by Figure 1.

Assuming that an N_c-length time-domain transmit block is represented by a vector $\mathbf{s} = [s(0), s(1), \ldots, s(N_c - 1)]^T$, PAPR of the time-domain transmit signal calculated over an oversampled transmission block is expressed by

DOI: 10.1002/wcm

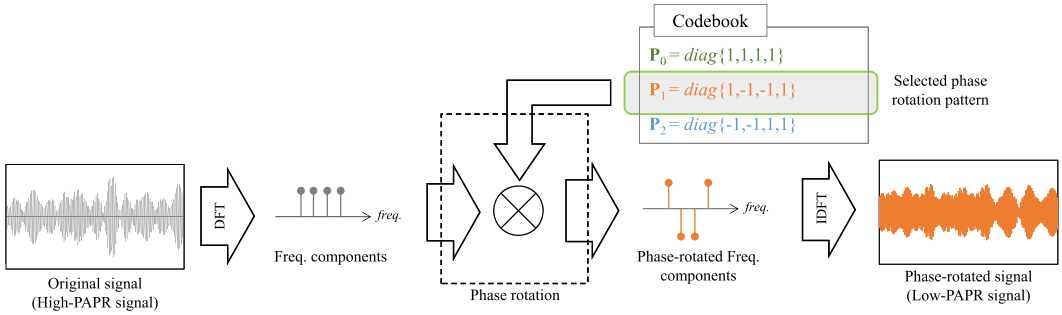

Figure 1. Signal processing in frequency-domain selected mapping.

$$\text{PAPR} = \frac{\max\left\{|s(n)|^2, n = 0, \frac{1}{V}, \frac{2}{V}, \ldots, N_c - 1\right\}}{\frac{1}{N_c}\sum_{n=0}^{N_c-1}|s(n)|^2}, \quad (1)$$

where V is oversampling factor.

According to Figure 1, a set of U different $N_c \times N_c$ diagonal matrices representing phase rotation pattern $\mathbf{P}_u = diag[P_u(0), \ldots, P_u(N_c-1)], u = 0 \sim U-1$ is defined. Candidates for the frequency-domain transmit signal block are generated by multiplying the phase-rotation matrix to the frequency-domain components after transmit filtering and before IDFT, represented by $\mathbf{S} = \mathbf{H}_T\mathbf{F}_{N_c}\mathbf{d}$, where $\mathbf{H}_T$ and $\mathbf{F}_{N_c}$ represent transmit filtering and N_c-point DFT operations, respectively. The vector $\mathbf{d} = [d(0), \ldots, d(N_c-1)]^T$ represents the time-domain transmit symbols block. The definitions of $\mathbf{H}_T$ and $\mathbf{F}_{N_c}$ will be described in details in Section 2.2.

In addition, the phase-rotation matrix for the first candidate $\mathbf{P}_0$ is set to be an $N_c \times N_c$ identity matrix $\mathbf{I}_{N_c}$ as a representative of original transmit block, where the other candidates are generated either in deterministic or random approach. We assume the phase rotation pattern to be real valued and unit magnitude, that is, $P_u(k) = \pm 1, k = 0 \sim N_c - 1$. The reason of setting $P_u(k)$ as real valued is to reduce the number of complex-valued multiplication of the transmitter, especially when the low-PAPR SC-FDE are expected to be exploited in uplink communication. The unit-magnitude property is required in order to meet transmit power constraint. In this paper, we use a set of phase rotation patterns generated randomly, which is confirmed in [17,18], where it provides the best PAPR reduction performance.

The instantaneous PAPR of transmit block candidates $\mathbf{s}_u = \mathbf{F}_{N_c}^H\mathbf{P}_u\mathbf{S}$ for all u are calculated by referencing (1), and the selected transmit signal $\mathbf{s}_{\hat{u}} = [s_{\hat{u}}(0), \ldots, s_{\hat{u}}(N_c - 1)]^T$ with the corresponding selected phase rotation pattern index $\hat{u}$ is selected by the following criterion:

$$\hat{u} = \arg\min_{u=0,1,\ldots,U-1} \text{PAPR}\left(\mathbf{s}_u = \mathbf{F}_{N_c}^H\mathbf{P}_u\mathbf{H}_T\mathbf{F}_{N_c}\mathbf{d}\right). \quad (2)$$

Note that the matrix and vector representations for transmit signal processing will be described in more details in Section 2.2.

2.2. Transceiver system model

Single-user N_c-length SC-FDE block transmission with N_g-length cyclic prefix (CP) insertion is considered in this paper. DFT and IDFT are employed in the transceiver for reaching frequency-domain processing, at which the transmit filtering and receive FDE can be applied as simple one-tap multiplication. The SC-FDE using FD-SLM transceiver is illustrated in Figure 2.

2.2.1. Transmitter.

Transmitter of SC-FDE equipped with FD-SLM is shown in Figure 2(a). We begin with a block consisting of N_c data-modulated symbols $\mathbf{d} = [d(0), \ldots, d(N_c-1)]^T$. The block $\mathbf{d}$ is transformed into frequency domain by N_c-point DFT, yielding the frequency-domain signal vector $\mathbf{D} = [D(0), \ldots, D(N_c-1)]^T$ as

$$\mathbf{D} = \mathbf{F}_{N_c}\mathbf{d}, \quad (3)$$

where the N_c-point DFT matrix $\mathbf{F}_{N_c}$ is given by

$$\mathbf{F}_{N_c} = \frac{1}{\sqrt{N_c}}\begin{bmatrix} 1 & 1 & \cdots & 1 \\ 1 & e^{\frac{-j2\pi(1)(1)}{N_c}} & \cdots & e^{\frac{-j2\pi(1)(N_c-1)}{N_c}} \\ \vdots & \vdots & \ddots & \vdots \\ 1 & e^{\frac{-j2\pi(N_c-1)(1)}{N_c}} & \cdots & e^{\frac{-j2\pi(N_c-1)(N_c-1)}{N_c}} \end{bmatrix}, \quad (4)$$

and its Hermitian transpose represents an inverse operation.

Next, $\mathbf{D}$ is multiplied by transmit filtering matrix $\mathbf{H}_T = diag[H_T(0), \ldots, H_T(N_c-1)]$. We assume the transmit filtering in this paper to be SRRC filtering with roll-off factor $\alpha = 0$, that is, ideal rectangular filtering, resulting in $H_T(k) = 1$ for all $k = 0 \sim N_c - 1$. The frequency-domain filtered signal is represented by

$$\mathbf{S} = \mathbf{H}_T\mathbf{F}_{N_c}\mathbf{d}. \quad (5)$$

The filtered signal $\mathbf{S}$ is then used as input signal in FD-SLM algorithm as described in Section 2.1 and Figure 1. The candidates are generated by multiplying $\mathbf{S}$ with $\mathbf{P}_u, u = 0 \sim U - 1$, following by IDFT

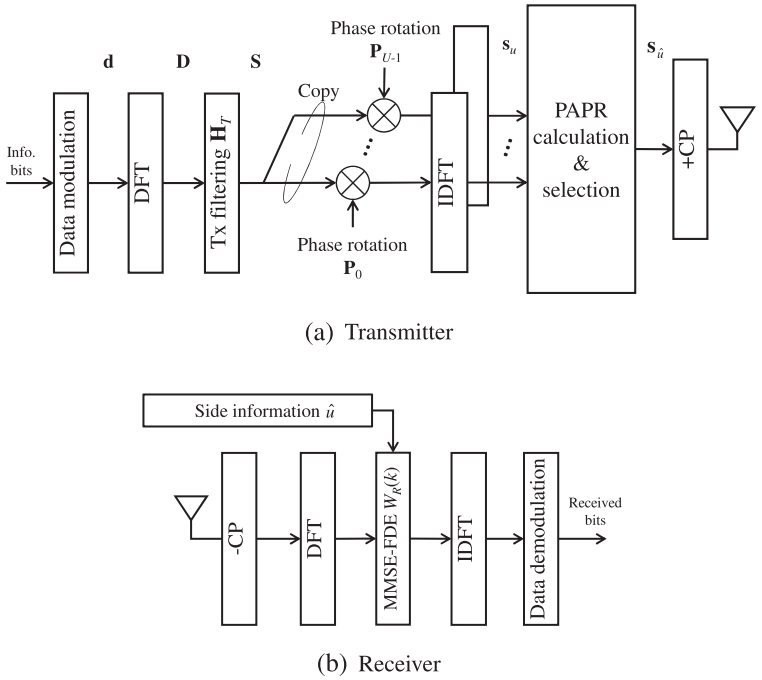

Figure 2. Transceiver system model of SC-FDE using FD-SLM. SC-FDE, single-carrier transmission with frequency-domain equalization; FD-SLM, frequency-domain selected mapping; DFT, discrete Fourier transform; IDFT, inverse DFT; PAPR, peak-to-average power ratio.

operation for obtaining the time-domain transmit block candidates $\mathbf{s}_u$. Selection is employed by referencing to (2) for obtaining the time-domain transmit block providing the lowest PAPR among U candidates, that is, $\mathbf{s}_{\hat{u}}$, together with the selected phase rotation pattern $\mathbf{P}_{\hat{u}}$. In summary, the time-domain transmit signal after passing through all processes $\mathbf{s}_{\hat{u}} = [s_{\hat{u}}(0), \ldots, s_{\hat{u}}(N_c - 1)]^T$ can be expressed as

$$\mathbf{s}_{\hat{u}} = \mathbf{F}_{N_c}^H \mathbf{P}_{\hat{u}} \mathbf{H}_T \mathbf{D} = \mathbf{F}_{N_c}^H \mathbf{P}_{\hat{u}} \mathbf{H}_T \mathbf{F}_{N_c} \mathbf{d}. \tag{6}$$

In case that $\mathbf{H}_T$ is SRRC filtering with roll-off factor $\alpha = 0$, (6) can be simplified as

$$\mathbf{s}_{\hat{u}} = \mathbf{F}_{N_c}^H \mathbf{P}_{\hat{u}} \mathbf{F}_{N_c} \mathbf{d}. \tag{7}$$

Finally, the last N_g samples of transmit block are copied as a CP and inserted into the guard interval, then a CP-inserted signal block of $N_g + N_c$ samples is transmitted.

2.2.2. Receiver.

The wireless propagation channel in this paper is assumed to be a symbol-spaced L-path frequency-selective block fading channel [2], where its impulse response is given by

$$h(\tau) = \sum_{l=0}^{L-1} h_l \delta(\tau - \tau_l), \tag{8}$$

where h_l and τ_l are complex-valued path gain and time delay of the l-th path, respectively. $\delta(\cdot)$ is the delta function. Time-domain received signal vector after CP removal $\mathbf{r}_{\hat{u}} = [r_{\hat{u}}(0), \ldots, r_{\hat{u}}(N_c - 1)]^T$ is expressed by

$$\mathbf{r}_{\hat{u}} = \sqrt{\frac{2E_s}{T_s}} \mathbf{h} \mathbf{s}_{\hat{u}} + \mathbf{n}, \tag{9}$$

where $\mathbf{s}_{\hat{u}} = \mathbf{F}_{N_c}^H \mathbf{P}_{\hat{u}} \mathbf{H}_T \mathbf{F}_{N_c} \mathbf{d}$ is obtained from (6). E_s is symbol energy, and $\mathbf{n}$ is noise vector in which each element is zero-mean additive white Gaussian noise having the variance $2N_0/T_s$ with T_s is symbol duration and N_0 being the one-sided noise power spectrum density. Channel response matrix $\mathbf{h}$ is a circular matrix representing time-domain channel response, which is

$$\mathbf{h} = \begin{bmatrix} h_0 & & & h_{L-1} & \cdots & h_1 \\ h_1 & \ddots & & & \ddots & \vdots \\ \vdots & & h_0 & \mathbf{0} & & h_{L-1} \\ h_{L-1} & & h_1 & \ddots & & \\ & \ddots & \vdots & & \ddots & \\ \mathbf{0} & & h_{L-1} & \cdots & \cdots & h_0 \end{bmatrix}. \tag{10}$$

The received signal is transformed into frequency domain by N_c-point DFT, obtaining the frequency-domain received signal vector $\mathbf{R}_{\hat{u}} = [R_{\hat{u}}(0), \ldots, R_{\hat{u}}(N_c - 1)]^T$ as

$$\begin{aligned}\mathbf{R} &= \sqrt{\frac{2E_s}{T_s}}\mathbf{F}_{N_c}\mathbf{h}\mathbf{s}_{\hat{u}} + \mathbf{F}_{N_c}\mathbf{n} \\ &= \sqrt{\frac{2E_s}{T_s}}\mathbf{F}_{N_c}\mathbf{h}\mathbf{F}_{N_c}^H\mathbf{P}_{\hat{u}}\mathbf{H}_T\mathbf{D} + \mathbf{F}_{N_c}\mathbf{n} \\ &= \sqrt{\frac{2E_s}{T_s}}\mathbf{H}_c\mathbf{P}_{\hat{u}}\mathbf{H}_T\mathbf{D} + \mathbf{N},\end{aligned} \tag{11}$$

where the frequency-domain channel response $\mathbf{H}_c$ is

$$\mathbf{F}_{N_c}\mathbf{h}\mathbf{F}_{N_c}^H = diag[H_c(0), \ldots, H_c(N_c-1)] \equiv \mathbf{H}_c. \tag{12}$$

Frequency-domain equalization based on minimum mean-square error criterion (MMSE-FDE) is multiplied to $\mathbf{R}_{\hat{u}}$ in order to mitigate the effect of frequency-selective fading. The FDE is represented by $N_c \times N_c$ diagonal matrix $\mathbf{W}_R = diag[W_R(0), \ldots, W_R(N_c-1)]$, which is equivalent to simple one-tap multiplication. The FDE weight with respect to each frequency index $W_R(k)$ are derived so as to minimize the mean-square error between frequency-domain transmit signal $\mathbf{D}$ (defined by (3)) and received signal $\hat{\mathbf{D}} = \mathbf{W}_R\mathbf{R}_{\hat{u}}$, yielding

$$W_R(k) = \frac{H_c^*(k)P_{\hat{u}}^*(k)H_T^*(k)}{|H_c(k)P_{\hat{u}}(k)H_T(k)|^2 + (E_s/N_0)^{-1}}. \tag{13}$$

It is observed from (13) that the information of channel response, transmit filtering coefficient, and the selected phase rotation pattern are indispensable. In general, the receiver knows $H_c(k)$ through channel estimation [19], where the transmit filtering coefficient is predetermined. To inform the receiver about the phase rotation pattern, at least $\log_2 U$ bits are required as a side information containing the pattern number. We assume the perfect channel estimation and ideal side information detection (i.e., error-free side information detection) in this paper for simplicity.

Finally, the frequency-domain equalized signal $\hat{\mathbf{D}} = \mathbf{W}_R\mathbf{R}_{\hat{u}}$ is transformed back into time domain by N_c-point IDFT. The time-domain received signal before demodulation $\hat{\mathbf{d}} = [\hat{d}(0), \ldots, \hat{d}(N_c-1)]^T$ is expressed by

$$\begin{aligned}\hat{\mathbf{d}} &= \mathbf{F}_{N_c}^H\mathbf{W}_R\mathbf{R}_{\hat{u}} \\ &= \sqrt{\frac{2E_s}{T_s}}\mathbf{F}_{N_c}^H\mathbf{W}_R\mathbf{H}_c\mathbf{P}_{\hat{u}}\mathbf{D} + \mathbf{F}_{N_c}^H\mathbf{W}_R\mathbf{N}.\end{aligned} \tag{14}$$

3. SC-FDE USING TD-SLM

In this section, an explanation of TD-SLM algorithm and its implementation in SC-FDE are provided. The TD-SLM algorithm is different from the FD-SLM because the generation of transmit block candidates (i.e., phase rotation) is employed in time domain. This also results in the difference between the transceivers of SC-FDE using TD-SLM and SC-FDE using FD-SLM.

3.1. TD-SLM algorithm

The TD-SLM algorithm and its signal processing are depicted in Figure 3. A set of U different $N_c \times N_c$ diagonal phase rotation pattern matrices $\mathbf{P}_u = diag[P_u(0), \ldots, P_u(N_c-1)], u = 0 \sim U-1$ is defined, which is similar to FD-SLM. However, $\mathbf{P}_u$ is multiplied to time-domain transmit symbols block $\mathbf{d}$ instead of in frequency domain, and then obtaining the time-domain candidate $\mathbf{d}_u = \mathbf{P}_u\mathbf{d}$. The pattern generation is exactly the same as in FD-SLM, that is, $P_u(n) = \pm 1, n = 0 \sim N_c - 1$ is generated in random approach. (Note that we use the time index n instead of frequency index k for emphasizing that phase rotation is applied in time domain.)

All of the time-domain block candidates in U branches are then passed through transmit signal processing (the details are described in Section 3.2). The instantaneous PAPR of time-domain transmit signal candidates after passing through transmit signal processing $\mathbf{s}_u = [s_u(0), \ldots, s_u(N_c-1)]^T$ are calculated based on (1), and the selected transmit signal $\mathbf{s}_{\hat{u}} = [s_{\hat{u}}(0), \ldots, s_{\hat{u}}(N_c-1)]^T$ with the corresponding selected phase rotation pattern index $\hat{u}$ is selected by the following criterion:

$$\hat{u} = \arg \min_{u=0,1,\ldots,U-1} \text{PAPR}\left(\mathbf{s}_u = \mathbf{F}_{N_c}^H\mathbf{H}_T\mathbf{F}_{N_c}\mathbf{P}_u\mathbf{d}\right). \tag{15}$$

It is observed that (15) is different from (2) because $\mathbf{P}_u$ is multiplied before DFT operation. Note that the matrix

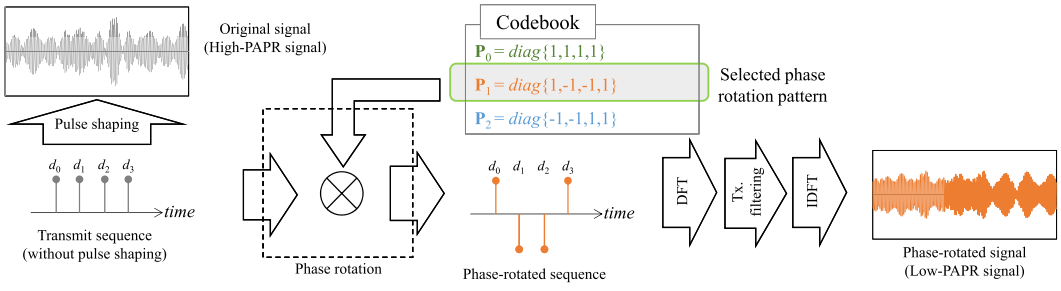

Figure 3. Signal processing in TD-SLM. TD-SLM, time-domain selected mapping; DFT, discrete Fourier transform; IDFT, inverse DFT; PAPR, peak-to-average power ratio.

and vector representations for transmit signal processing in (15) will be described in more details in Section 3.2.

3.2. Transceiver system model

Similar to Section 2.2, single-user N_c-length block transmission with N_g-length of CP insertion is assumed. In a system using TD-SLM, time-domain symbols are mapped by multiplying with phase rotation pattern prior to applying DFT. Transceiver system model of SC-FDE using TD-SLM is shown in Figure 4.

3.2.1. Transmitter.

Transmitter of SC-FDE using TD-SLM is shown in Figure 4(a). A transmit block consisting of N_c data-modulated symbols $\mathbf{d} = [d(0), \ldots, d(N_c - 1)]^T$ is used for generating U candidates for SLM $\mathbf{d}_u$ by multiplying with different phase rotation pattern. The u-th transmit block candidate is expressed by

$$\mathbf{d}_u = \mathbf{P}_u \mathbf{d}, \tag{16}$$

where $\mathbf{P}_u = diag\,[P_u(0), \ldots, P_u(N_c - 1)]$ represents phase rotation pattern matrix. The detail of phase rotation pattern generation is already discussed in Section 3.1. Then, each transmit block candidate is transformed into frequency domain by N_c-point DFT, yielding frequency-domain transmit signal of the u-th candidate $\mathbf{D}_u = [D_u(0), \ldots, D_u(N_c - 1)]^T$ as

$$\mathbf{D}_u = \mathbf{F}_{N_c} \mathbf{P}_u \mathbf{d}, \tag{17}$$

where N_c-point DFT matrix $\mathbf{F}_{N_c}$ is already defined in (4).

Next, $\mathbf{D}_u$ is multiplied by the transmit filtering matrix $\mathbf{H}_T = diag\,[H_T(0), \ldots, H_T(N_c - 1)]$, obtaining the frequency-domain signal after filtering for the u-th candidate $\mathbf{S}_u = \mathbf{H}_T \mathbf{D}_u$. Note that the SRRC filtering with roll-off factor $\alpha = 0$ is assumed for the transmit filtering, similar to SC-FDE using FD-SLM.

After that, $\mathbf{S}_u$ is transformed back into time domain by N_c-point IDFT $\mathbf{F}_{N_c}^H$. PAPR calculation is applied in order to search and select the time-domain transmit signal with the lowest PAPR based on (15), yielding $\mathbf{s}_{\hat{u}} = [s_{\hat{u}}(0), \ldots, s_{\hat{u}}(N_c - 1)]^T$. The selected time-domain transmit signal based on TD-SLM is expressed by

$$\mathbf{s}_{\hat{u}} = \mathbf{F}_{N_c}^H \mathbf{H}_T \mathbf{F}_{N_c} \mathbf{d}_{\hat{u}} = \mathbf{F}_{N_c}^H \mathbf{H}_T \mathbf{F}_{N_c} \mathbf{P}_{\hat{u}} \mathbf{d}. \tag{18}$$

In addition, if $\mathbf{H}_T$ is SRRC filtering with roll-off factor $\alpha = 0$, (18) can be simplified as

$$\mathbf{s}_{\hat{u}} = \mathbf{P}_{\hat{u}} \mathbf{d}. \tag{19}$$

Finally, the last N_g samples of transmit block are copied as a CP and inserted into the guard interval, then a CP-inserted signal block of $N_g + N_c$ samples is transmitted.

3.2.2. Receiver.

The propagation channel is assumed to be the same as in Section 2.2, that is, a symbol-spaced L-path frequency-selective block fading channel [2], where its impulse response and channel response matrix are represented by

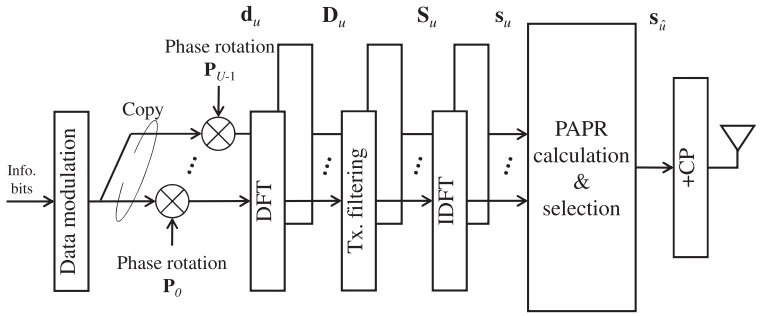

(a) Transmitter

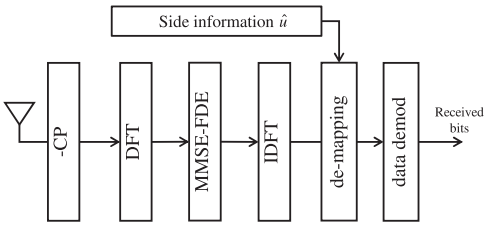

(b) Receiver

Figure 4. Transceiver system model of SC-FDE using TD-SLM. SC-FDE, single-carrier transmission with frequency-domain equalization; TD-SLM, time-domain selected mapping; DFT, discrete Fourier transform; IDFT, inverse DFT; PAPR, peak-to-average power ratio.

(8) and (10), respectively. The time-domain received signal vector after CP removal $\mathbf{r}_{\hat{u}} = [r_{\hat{u}}(0), \ldots, r_{\hat{u}}(N_c - 1)]^T$ is expressed by

$$\mathbf{r}_{\hat{u}} = \sqrt{\frac{2E_s}{T_s}}\mathbf{h}\mathbf{s}_{\hat{u}} + \mathbf{n}, \tag{20}$$

where $\mathbf{s}_{\hat{u}} = \mathbf{F}_{N_c}^H \mathbf{H}_T \mathbf{F}_{N_c} \mathbf{P}_{\hat{u}} \mathbf{d}$ is obtained from (18). The received signal vector $\mathbf{r}_{\hat{u}}$ is transformed into frequency domain by N_c-point DFT, obtaining the frequency-domain received signal $\mathbf{R}_{\hat{u}}$ as

$$\begin{aligned}\mathbf{R}_{\hat{u}} &= \sqrt{\frac{2E_s}{T_s}}\mathbf{F}_{N_c}\mathbf{h}\mathbf{F}_{N_c}^H \mathbf{H}_T \mathbf{D}_{\hat{u}} + \mathbf{F}_{N_c}\mathbf{n} \\ &= \sqrt{\frac{2E_s}{T_s}}\mathbf{H}_c \mathbf{H}_T \mathbf{D}_{\hat{u}} + \mathbf{N},\end{aligned} \tag{21}$$

where $\mathbf{H}_c$ is already defined in (12).

MMSE weight matrix $\mathbf{W}_R = diag[W_R(0), \ldots, W_R(N_c - 1)]$ is applied at the receiver in order to reduce the effect from frequency selectivity. The equalized signal $\hat{\mathbf{D}}_{\hat{u}} = \mathbf{W}_R \mathbf{R}_{\hat{u}}$ is obtained, where $W_R(k)$ is determined by

$$W_R(k) = \frac{H_c^*(k) H_T^*(k)}{|H_c(k) H_T(k)|^2 + (E_s/N_0)^{-1}}. \tag{22}$$

It is observed that the MMSE-FDE weight in (22) is different from (13) because the selected phase rotation pattern $\mathbf{P}_u$ is not considered; meanwhile, the de-mapping is employed in time domain instead.

The frequency-domain equalized signal $\hat{\mathbf{D}}_{\hat{u}}$ is then transformed back into time domain by N_c-point IDFT, yielding time-domain equalized signal vector before applying de-mapping $\tilde{\mathbf{d}}_{\hat{u}} = [\tilde{d}_{\hat{u}}(0), \ldots, \tilde{d}_{\hat{u}}(N_c - 1)]^T$ as

$$\begin{aligned}\tilde{\mathbf{d}}_{\hat{u}} &= \mathbf{F}_{N_c}^H \hat{\mathbf{D}}_{\hat{u}} \\ &= \sqrt{\frac{2E_s}{T_s}}\mathbf{F}_{N_c}^H \mathbf{W}_R \mathbf{R}_{\hat{u}} + \mathbf{F}_{N_c}^H \mathbf{W}_R \mathbf{N}.\end{aligned} \tag{23}$$

Finally, de-mapping is applied in order to obtain the original time-domain transmit block. De-mapping is simply performed by multiplying the time-domain equalized signal with the Hermitian transpose of selected phase rotation pattern matrix, obtaining time-domain received vector $\hat{\mathbf{d}} = [\hat{d}(0), \ldots, \hat{d}(N_c - 1)]^T$ as

$$\hat{\mathbf{d}} = \mathbf{P}_{\hat{u}}^H \tilde{\mathbf{d}}_{\hat{u}}. \tag{24}$$

Similar to FD-SLM, it is observed from (24) that the receiver needs to know which phase rotation pattern is selected at the transmitter; otherwise, de-mapping cannot be organized accurately and consequently leads to BER degradation. This indicates that explicit side information transmission is also indispensable in TD-SLM.

In summary, the similarity and difference among conventional SLM technique in OFDM transmission [12], the proposed FD-SLM, and TD-SLM for SC-FDE transmission can be described as follows.

- The main concept of the conventional SLM technique in OFDM transmission and the proposed SLM techniques for SC-FDE are similar; in other words, those SLM techniques aim to increase the degree-of-freedom of PAPR of transmit signal by generating the transmit signal candidates by multiplying the various phase rotation patterns to the original signal.
- However, candidate generation and the places where the multiplication of phase rotation pattern are carried out for each SLM techniques are different. For example, in OFDM transmission, phase rotation pattern is multiplied to frequency components where each component contains data-modulated symbol. In SC-FDE transmission using FD-SLM, phase rotation pattern multiplication is applied to frequency components, but each component contains the DFT-precoded data-modulated symbols. In contrast, phase rotation pattern multiplication is applied directly to time-domain data-modulated symbol (not subcarrier) in SC-FDE using TD-SLM. We also would like to mention that the original SLM method for OFDM signal does not employ phase rotation pattern multiplication in time domain.

In addition, we would like to leave the computational complexity problem as our future work because the problems of PAPR reduction is considered as higher priority than computational complexity.

4. PERFORMANCE EVALUATION

Numerical and simulation parameters are summarized in Table I. We assume 4 QAM, 16 QAM, and 64 QAM SC block transmission with the number of available subcarriers $N_c = 64$. Oversampling factor for PAPR evaluation is assumed to be $V = 8$. System performances of conventional SRRC filtered SC-FDE, SC-FDE using FD-SLM, and SC-FDE using TD-SLM are evaluated in terms of PAPR of transmit signal, average BER (uncoded), throughput, and computational complexity.

4.1. Peak-to-average power ratio

The complementary cumulative distribution function (CCDF) of PAPR was first obtained. Then, the PAPR value at CCDF = 0.001, called $\text{PAPR}_{0.1\%}$, is found and discussed.

Figure 5 shows the $\text{PAPR}_{0.1\%}$ performances of SC-FDE using FD-SLM and SC-FDE using TD-SLM, as a function of number of candidates (U) and with various data modulation levels. The original SC-FDE mentioned in this

Table I. Simulation parameters.

Transmitter	Data modulation	4 QAM, 16 QAM, 64 QAM
	No. of subcarriers	$N_c = 64$
	Cyclic prefix length	$N_g = 16$
	Transmit filtering	SRRC (α=0, 0.22)
	Phase rotation sequence type	Random
	No. of candidates	$U = 1 \sim 512$
	$PAPR_{0.1\%}$ threshold	6 dB
Channel	Fading type	Frequency-selective block Rayleigh
	Power delay profile	Symbol-spaced 16-path uniform
	Channel estimation	Ideal
Receiver	Side information sharing	Ideal detection
	FDE	MMSE-FDE

QAM, quadrature amplitude modulation; PAPR, peak-to-average power ratio; FDE, frequency-domain equalization; MMSE-FDE, frequency-domain equalization based on minimum mean-square error criterion.

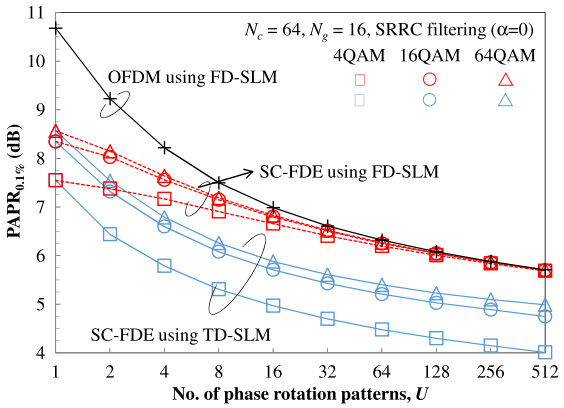

Figure 5. PAPR versus the number of phase rotation patterns. SC-FDE, single-carrier transmission with frequency-domain equalization; TD-SLM, time-domain selected mapping; FD-SLM, frequency-domain SLM; PAPR, peak-to-average power ratio; QAM, quadrature amplitude modulation; OFDM, orthogonal frequency division multiplexing.

paper refers to the DFT-precoded SC-FDE; in other words, the transmit signal processing is carried out by inserting the DFT into the conventional CP-inserted OFDM transmitter. The SC-FDE signal produced by inserting DFT as a precoder into the OFDM transmitter is used in Long-Term Evolution wireless network [20]. Its PAPR value is equal to the case when $U = 1$ (equivalent to transmission without SLM) in Figure 5. The $PAPR_{0.1\%}$ of conventional SC-FDE is 7.5 dB for 4 QAM, 8.4 dB for 16 QAM, and 8.6 dB for 64 QAM. For comparison and analysis on PAPR of SC-FDE signals, the $PAPR_{0.1\%}$ of OFDM transmission using FD-SLM assuming 16 QAM modulation is plotted. TD-SLM is not available for OFDM signals because time-domain signal after IDFT is already pulse shaped and there is no change on PAPR when phase rotation pattern is multiplied. The CCDF of PAPR of OFDM signal can be approximated by using the central limit theorem to assume that the real and imaginary parts of time-domain signal follow a Gaussian distribution [12,21], where the CCDF can be expressed by $prob(\text{PAPR} > z) \approx 1 - (1 - e^{-z})^{\beta N_c}$. Here, N_c represents the number of subcarriers and β is an approximation parameter for oversampling, which is set to be $\beta = 2.3$ [22]. The CCDF of PAPR of OFDM using FD-SLM can be approximated by assuming that all the phase-rotated transmit blocks are independent to each other and is expressed by $prob(\text{PAPR}_{\text{FD-SLM}} > z) \approx [1 - (1 - e^{-z})^{\beta N_c}]^U$, where U is the number of phase rotation patterns [22].

In addition, it is shown in [12,13] that the SLM can effectively reduce the PAPR of OFDM signal with moderate computational complexity and its PAPR-complexity trade-off is much better than partial transmit sequence technique [14]. Therefore, SLM can be considered as a strong candidate among other PAPR reduction techniques for OFDM transmission and consequently has potential to be a promising PAPR reduction technique for SC-FDE signal. To the best knowledge of the authors, the PAPR reduction for SC-FDE has not been extensively examined except the use of transmit filtering [6–9]. Therefore, in this paper, the SRRC filter [6] is used as a reference in performance comparison.

It is observed from Figure 5 that $PAPR_{0.1\%}$ decreases when U increases in OFDM using FD-SLM, SC-FDE using FD-SLM, and TD-SLM. It can be seen that more than 3 dB reduction of PAPR compared with the original SC-FDE can be achieved when $U = 512$. This is because increasing U leads to an increasing of degree-of-freedom, and hence results in higher probability to obtain a low-PAPR signal from transmit candidates. In addition, there are two more observations obtained from the results in Figure 5: the first one is the $PAPR_{0.1\%}$ of OFDM using FD-SLM and SC-FDE using FD-SLM becomes converging to the same value when U is large, and the second one is TD-SLM outperforms FD-SLM by achieving lower PAPR in every modulation level and number of phase rotation patterns. The reasons for supporting the aforementioned two observations can be analyzed by referring the following computer simulation results.

Figure 6 shows the CDF of PAPR reduction effects defined by the difference between the PAPR of the transmit signal, which is phase rotated by the selected phase rotation pattern (i.e., SLM output signal) and that of the original transmit signal, that is, $\text{PAPR}(\mathbf{s}_{\hat{u}}) - \text{PAPR}(\mathbf{s})$, where $\mathbf{s}_{\hat{u}}$ is defined in (6) and (18). The number of phase rotation patterns is assumed to be $U = 64$ and assuming 16 QAM modulation. It is obviously seen that the OFDM using FD-SLM achieves the best PAPR reduction performance,

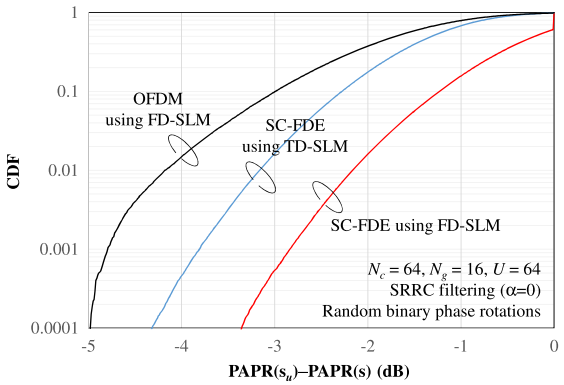

Figure 6. CDF of PAPR reduction. SC-FDE, single-carrier transmission with frequency-domain equalization; TD-SLM, time-domain selected mapping; FD-SLM, frequency-domain SLM; PAPR, peak-to-average power ratio; CDF, cumulative distribution function; OFDM, orthogonal frequency division multiplexing; SRRC, square-root raised-cosine.

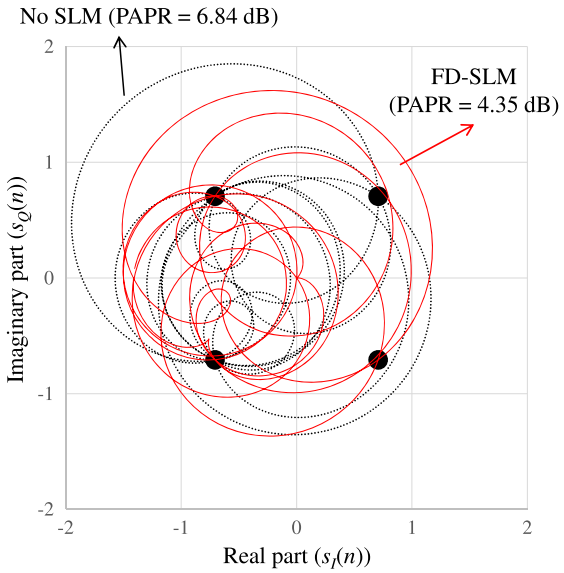

4QAM modulation, N_c = 16, U=64
SRRC filtering (α=0), Random binary phase rotations

(a) SC-FDE using FD-SLM

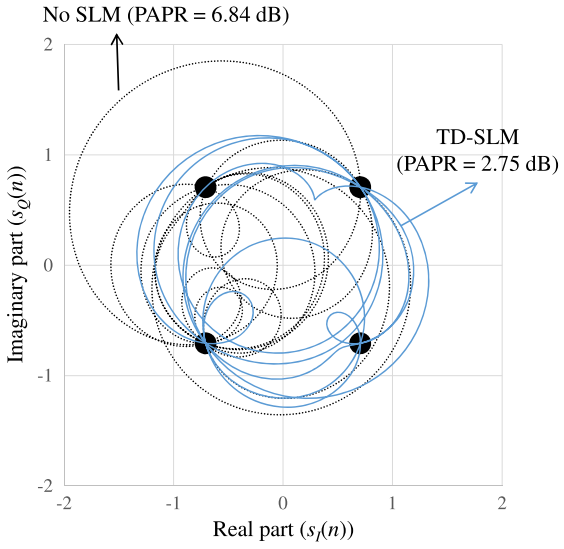

4QAM modulation, N_c = 16, U=64
SRRC filtering (α=0), Random binary phase rotations

(b) SC-FDE using TD-SLM

Figure 7. Complex envelope of the SC-FDE using SLM. SC-FDE, single-carrier transmission with frequency-domain equalization; TD-SLM, time-domain selected mapping; FD-SLM, frequency-domain SLM; PAPR, peak-to-average power ratio; SRRC, square-root raised-cosine.

following by the SC-FDE using TD-SLM and SC-FDE using FD-SLM, respectively. The result in Figure 6 is consistent with Figure 5 as the OFDM using FD-SLM can significantly reduce the PAPR as up to 4.3 dB of PAPR reduction is achievable, while up to 2.0 and 3.1 dB of PAPR reduction are achievable in SC-FDE using FD-SLM and TD-SLM, respectively. The reason is because the original OFDM signal has high PAPR, resulting in higher probability to obtain a phase rotation pattern among U patterns, which can reduce the PAPR. On the other hand, there is probability that no phase rotation pattern can reduce the PAPR among U patterns in SC-FDE because the original SC-FDE signal has low PAPR. The phenomenon that there is no phase rotation pattern among U patterns, can reduce the PAPR is obviously seen in SC-FDE using FD-SLM as the probability that the reduction efficiency is 0 dB is approximately 30%.

Figure 7 shows the complex envelope of transmit signal $s_{\hat{u}}(n) = s_{\hat{u},I}(n) + js_{\hat{u},Q}(n)$, where $s_{\hat{u}}(n)$ is the n-th element in $\mathbf{s}_{\hat{u}}$ defined in (6) and (18), in I-Q plane assuming $U = 64$, $N_c = 16$, and 4 QAM modulation. The transmit complex envelope of conventional SC-FDE, SC-FDE using FD-SLM, and SC-FDE using TD-SLM are plotted from the same set of data-modulated symbols. It is seen from both Figure 7(a) and (b) that the complex envelope of SC-FDE using FD-SLM and TD-SLM travel in narrower range compared with that of the conventional SC-FDE, resulting in lower peak amplitude and lower PAPR. In addition, it is seen that the complex envelope of SC-FDE using TD-SLM always pass through the original transmit signal constellations (here is 4 QAM constellations), where some parts of SC-FDE using FD-SLM does not pass through the original constellations. This is because applying phase rotation to SC-FDE signal in time domain always results in the phase-rotated signal which maintain original modulation scheme, for example, applying the phase rotation to 4 QAM data-modulated transmit block always obtains 4 QAM data-modulated symbols. By maintaining the original modulation level, the amplitude of resulting phase-rotated signal is bounded, and then, candidate generation via multiplication of phase rotation patterns can reach the nearly optimal solution, while the amplitude of

Table II. Optimal U for SLM algorithm.

		4 QAM	16 QAM	64 QAM
$PAPR_{0.1\%} \leq$ 6 dB	FD-SLM	U =128 (6.0 dB)	U = 256 (5.86 dB)	U = 256 (5.87 dB)
	TD-SLM	U = 4 (5.97 dB)	U = 16 (5.88 dB)	U = 16 (5.99 dB)
$PAPR_{0.1\%} \leq$ 4 QAM(7.55 dB)	FD-SLM	–	U = 4 (7.54 dB)	U = 8 (7.19 dB)
	TD-SLM	–	U = 2 (7.53 dB)	U = 4 (6.97 dB)
$PAPR_{0.1\%} \leq$ SRRC filtered SC-FDE w/ α=0.22 (4.3 dB for 4 QAM, 6.44 dB for 16 QAM, 6.96 dB for 64 QAM)	FD-SLM	$U \geq 512$	U = 64 (6.25 dB)	U = 16 (6.83 dB)
	TD-SLM	U = 256 (4.29 dB)	U = 8 (6.27 dB)	U = 4 (6.95 dB)

SLM, selected mapping; TD-SLM, time-domain SLM; FD-SLM, frequency-domain SLM; QAM, quadrature amplitude modulation; PAPR, peak-to-average power ratio; SC-FDE, single-carrier transmission with frequency-domain equalization; SRRC, square-root raised-cosine.

phase-rotated signal in SC-FDE using FD-SLM becomes close to Gaussian random variable (similar to OFDM using FD-SLM). Regarding to the aforementioned discussion, SC-FDE using TD-SLM has potential to achieve lower PAPR than FD-SLM.

In general, an optimal U for achieving a particular $PAPR_{0.1\%}$ value needs to be discussed to avoid insufficient computational complexity and side information bits. In this paper, the optimal U for achieving a particular $PAPR_{0.1\%}$ value is discussed in three approaches: the optimal U for achieving $PAPR_{0.1\%} \leq 6$ dB, the optimal U for keeping the $PAPR_{0.1\%}$ of multi-level modulated SC-FDE to be less than or equal to that of 4 QAM-modulated SC-FDE, and the optimal U for keeping the $PAPR_{0.1\%}$ to be less than or equal to that of SRRC filtered SC-FDE with $\alpha = 0.22$. The optimal U for those three aspects are shown in Table II, where the TD-SLM gives lower U than FD-SLM in every comparison.

Figure 8 shows the $PAPR_{0.1\%}$ performance comparison between SLM using real-valued phase rotation pattern (i.e., e^{j0} and $e^{j\pi}$) and SLM using complex-valued phase rotation. We assume 16 QAM modulation, while complex-valued phase rotation with phase rotation interval of 90° (i.e., $e^{j\theta}$ where $\theta = 0, \pm\pi/2, \pi$) and 45° (i.e., $e^{j\theta}$ where $\theta = 0, \pm\pi/4, \pm\pi/2, \pi$) are used for comparison. It is obviously seen in Figure 8 that there is no difference of $PAPR_{0.1\%}$ performance even though the phase rotation pattern is real valued or complex valued in both FD-SLM and TD-SLM. This result is also consistent with [18] and assuming OFDM transmission that the SLM provides the best performance when the phase rotation is discrete and uniformly distributed over $[0, 2\pi)$. Regarding to this simulation result, the use of real-valued phase rotation is attractive because it can reduce the unnecessary complex-valued multiplication operation because of candidate generation without degrading PAPR performance.

4.2. BER performance

To confirm that the proposed SLM algorithms for SC-FDE provide BER preservation property, BER perform a function of average received bit energy-to-noise power spectrum density ratio $E_b/N_0 = (1/N_{\mathrm{mod}})(E_s/N_0)(1 + N_g/N_c)$, where N_{mod} represents modulation level (two for 4 QAM, four for 16 QAM, and six for 64 QAM), of SC-FDE using FD-SLM and TD-SLM at $U = 512$ are shown in Figure 9 and compared with conventional SC-FDE.

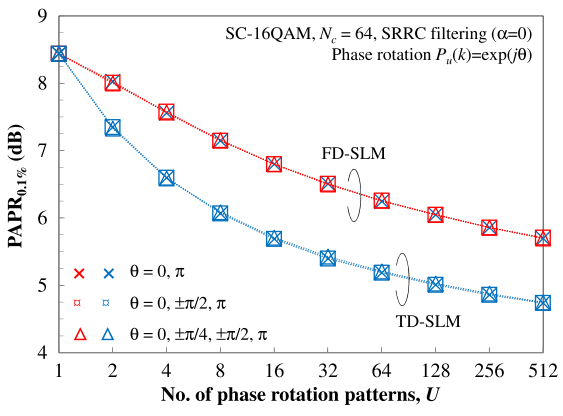

Figure 8. PAPR performance of complex-valued phase rotation patterns. TD-SLM, time-domain selected mapping; FD-SLM, frequency-domain SLM; PAPR, peak-to-average power ratio; SRRC, square-root raised-cosine; QAM, quadrature amplitude modulation.

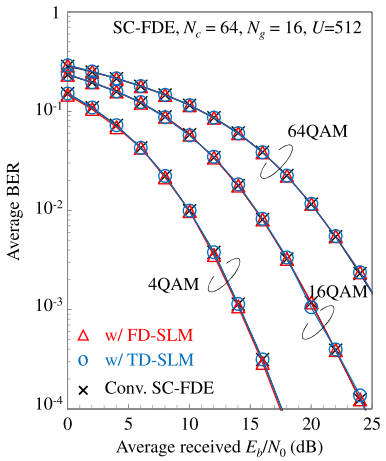

Figure 9. BER performances. SC-FDE, single-carrier transmission with frequency-domain equalization; TD-SLM, time-domain selected mapping; FD-SLM, frequency-domain SLM; BER, bit-error rate; QAM, quadrature amplitude modulation.

Ideal side information detection is assumed in this paper. It is obviously seen from Figure 9 that the BER performances of conventional SC-FDE, SC-FDE using FD-SLM, and SC-FDE using TD-SLM are the same, indicating that the SLM algorithms can reduce the PAPR without degrading the BER.

To achieve the BER preservation property, however, up to $\log_2 U$-bit of side information needs to be transmitted in order to achieve an accurate de-mapping at the receiver. The side information should be coded by using forward error-correction coding. However, this further degrades the throughput [23]. The impact of side information on throughput performance will be discussed in the next subsection.

4.3. Throughput performance

In this subsection, the throughput performances of SC-FDE using SLM algorithms are initially evaluated by average throughput performance as a function of peak transmit E_s/N_0, where the throughput performance in bps/Hz is defined as follows [24];

$$\eta = N_{\text{mod}} \times (1 - \text{PER}) \times \frac{1}{1+\alpha} \times \frac{1}{1+\frac{N_g+N_{SI}}{N_c}}, \quad (25)$$

where PER is packet-error rate and N_{SI} is the number of required side information symbols, which is assumed to be $N_{SI} = \lceil (\log_2 U)/N_{\text{mod}} \rceil$. Uncoded side information transmission and ideal side information detection are assumed for simplicity. The packet length is assumed to be 3072 bits in this paper. The peak transmit E_s/N_0 is considered because it refers to the required peak transmit power of a power amplifier, while the peak transmit E_s/N_0 is defined as a summation of average received E_s/N_0 and $\text{PAPR}_{0.1\%}$ [5].

Figure 10 shows the throughput performances as a function of peak transmit E_s/N_0 of the conventional SC-FDE, SRRC filtered SC-FDE with $\alpha = 0.22$, and SC-FDE using the proposed SLM. The number of candidates for both TD-SLM and FD-SLM are set as the minimum U for keeping the $\text{PAPR}_{0.1\%}$ to be less than or equal to that of SRRC filtered SC-FDE with $\alpha = 0.22$ (Table II), except in case of 4 QAM-modulated SC-FDE using FD-SLM where U is set to be 512 (the maximum value considered in this paper).

In Figure 10(a), it can be observed from the figure that SRRC filtered SC-FDE with $\alpha = 0.22$ achieves better throughput performance because of its low-PAPR property. However, its peak throughput degrades by a factor of $1/(1+\alpha)$. SC-FDE using FD-SLM can provide similar throughput performance at low peak E_s/N_0 region compared with SRRC filtered SC-FDE with $\alpha = 0.22$ (except in 4 QAM case), where there is a slight peak throughput degradation as a result from side information.

In Figure 10(b), it is seen that SC-FDE using TD-SLM provides similar throughput performance to SRRC filtered SC-FDE with $\alpha = 0.22$ at low peak E_s/N_0 region in every modulation scheme. TD-SLM requires less number of candidates (U) than FD-SLM for achieving the same PAPR performance, which is equivalent to less side information bits. This contributes to improving the peak throughput, even though the resulting peak throughput is still slightly less than conventional SC-FDE.

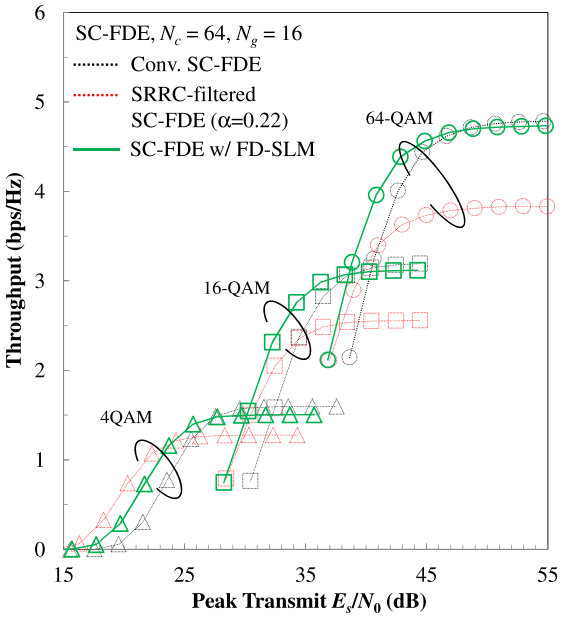

(a) FD-SLM

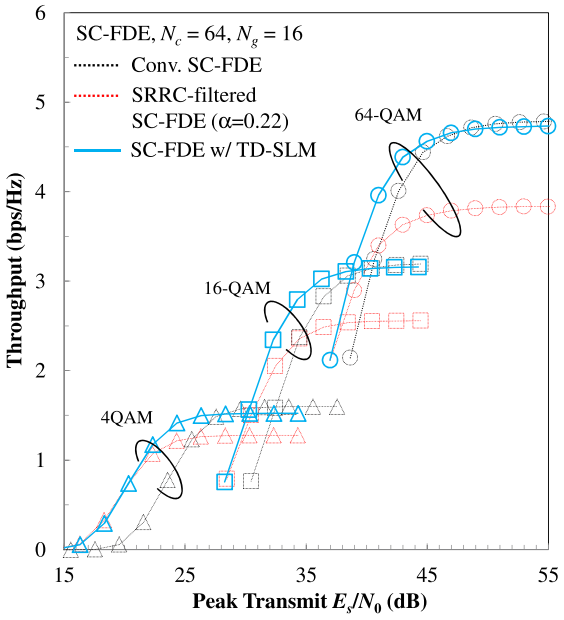

(b) TD-SLM

Figure 10. Throughput performances. SC-FDE, single-carrier transmission with frequency-domain equalization; TD-SLM, time-domain selected mapping; FD-SLM, frequency-domain SLM; SRRC, square-root raised-cosine; QAM, quadrature amplitude modulation.

Table III. Computational complexity performance.

	Conv. SC-FDE	SC-FDE with FD-SLM	SC-FDE with TD-SLM
Phase rotation	-	-	-
DFT	$(N_c)^2$	$(N_c)^2$	$U(N_c)^2$
IFFT	$N_c log_2(N_c)$	$UVN_c \log_2(VN_c)$	$UVN_c \log_2(VN_c)$
PAPR calculation	-	UVN_c	UVN_c

SC-FDE, single-carrier transmission with frequency-domain equalization; TD-SLM, time-domain selected mapping; FD-SLM, frequency-domain SLM; PAPR, peak-to-average power ratio; DFT, discrete Fourier transform; IFFT, inverse fast Fourier transform.

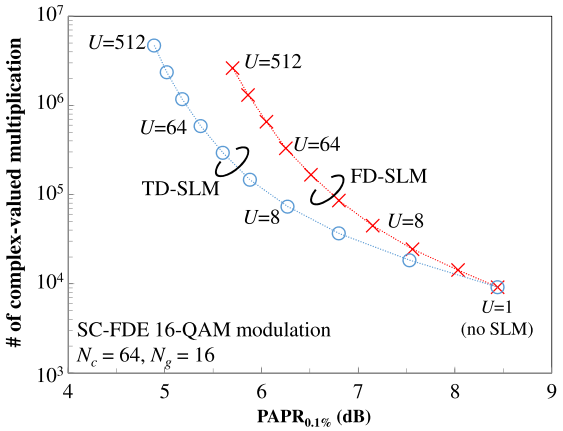

Figure 11. Computational complexity versus PAPR performance. SC-FDE, single-carrier transmission with frequency-domain equalization; TD-SLM, time-domain selected mapping; FD-SLM, frequency-domain SLM; PAPR, peak-to-average power ratio; QAM, quadrature amplitude modulation.

4.4. Computational complexity

The computational complexity performance is evaluated by counting the number of complex-valued multiplication [25]. Computational complexity as a function of the number of subcarriers (N_c) and candidates (U) for conventional SC-FDE, SC-FDE using FD-SLM, and SC-FDE using TD-SLM is summarized in Table III. Note that IDFT can be replaced by inverse fast Fourier transform (IFFT) if the number of subcarriers is a power of two.

It is seen from Table III, and indicated in [12,13], that SLM requires high computational complexity compared with the conventional SC-FDE because of the requirement of additional IFFT operations. SC-FDE using TD-SLM has more complexity at the same number of candidates compared with FD-SLM because it also requires additional DFT operations (typically U times of DFT operations compared with FD-SLM). In addition, the use of real-valued phase rotation pattern can reduce unnecessary computational complexity for generating the transmit waveform candidates.

However, the PAPR in Figure 5 shows that TD-SLM achieves similar PAPR to FD-SLM with less number of candidates. Figure 11 shows the $PAPR_{0.1\%}$ against complexity as a function of U for SC-FDE using FD-SLM and TD-SLM, assuming 16-QAM modulation. TD-SLM outperforms FD-SLM in terms of computational complexity when the required PAPR is set to be the same because TD-SLM requires less number of candidates. For example, at the point that $PAPR_{0.1\%}$=6 dB, TD-SLM requires only 10% of total computational complexity of FD-SLM.

5. CONCLUSION

In this paper, two spectrum-efficient PAPR reduction techniques for SC signals called FD-SLM and TD-SLM were proposed. The proposed techniques are based on generating transmit block candidates through phase rotation in different domains. The phase rotation is applied to subcarriers either between DFT and IFFT for FD-SLM, or directly to the time-domain transmit signal vector prior to DFT for TD-SLM. Simulation results confirmed that both FD-SLM and TD-SLM can efficiently reduce the PAPR of SC-FDE transmission without significant degradation on BER and throughput compared with SRRC filtered SC-FDE transmission. It was also clarified in this paper that the TD-SLM achieves better PAPR reduction performance compared with FD-SLM, at which the TD-SLM requires less number of candidates and less computational complexity than FD-SLM for achieving the same target PAPR.

ACKNOWLEDGEMENTS

This paper includes a part of results of “The research and development project for realization of the fifth-generation mobile communications system” (#0155-0019, April 2016) commissioned to Tohoku University and The Ministry of Internal Affairs and Communications (MIC), Japan.

REFERENCES

1. Adachi F, Takeda K, Yamamoto T, Matsukawa R, Kumagai S. Recent advances in single-carrier distributed antenna network. *Wiley Wireless Communication and Moblie Comput* 2011; **11**: 1551–1563.
2. Goldsmith A. *Wireless Communications*. Cambridge University Press: New York, 2005.

3. Han SH, Lee JH. An overview of peak-to-average power ratio reduction techniques for multicarrier transmission. *IEEE Transactions on Wireless Communications* 2005; **12**(2): 56–65.
4. Falconer D, Ariyavisitakul SL, Benyamin-Seeyar A, Edison B. Frequency domain equalization for single-carrier broadband wireless systems. *IEEE Communications Magazine* 2002; **40**(4): 58–66.
5. Okuyama S, Takeda K, Adachi F. MMSE frequency-domain equalization using spectrum combining for nyquist filtered broadband single-carrier transmission. In *Proceedings IEEE Vehicular Technology Conference (VTC 2010-Spring)*, Taipei, Taiwan, May 2010.
6. Akaiwa Y. *Introduction to Digital Mobile Communication* (1st edn). Wiley: New Jersey, 1997.
7. Rha P, Hsu S. Peak-to-average ratio (PAR) reduction by pulse shaping using a new family of generalized raised cosine filter. In *Proceedings IEEE Vehicular Technology Conference (VTC 2003-Fall),* Florida, USA, Oct. 2003; 706–710.
8. Meza C, Lee K, Lee K. PAPR Reduction in single carrier FDMA uplink system using parametric linear pulses. In *Proceedings International Conference on ICT Convergence (ICTC 2011)*, Seoul, Korea, Sept. 2011; 424–429.
9. Boonkajay A, Obara T, Yamamoto T, Adachi F. Excess-bandwidth transmit filtering based on minimization of variance of instantaneous transmit power for low-PAPR SC-FDE. *IEICE Transactions on Communications* 2015; **E98-B**(04): 673–685.
10. Li X, Cimini LJ. Effects of clipping and filtering on the performance of OFDM. *IEEE Communications Letters* 1998; **2**(5): 131–133.
11. Carson N, Gulliver TA. PAPR reduction of OFDM using selected mapping, modified RA codes and clipping. In *Proceedings IEEE Vehicular Technology Conference (VTC 2002-Fall)*, Vancouver, Canada, Sept. 2002; 1070–1073.
12. Bauml RW, Fischer RFH, Huber JB. Reducing the peak-to-average power ratio of multicarrier modulation by selected mapping. *IEEE Electronics Letters* 1996; **32**(22): 2056–2057.
13. Gacanin H, Adachi F. Selective mapping with symbol re-mapping for OFDM/TDM using MMSE-FDE. In *Proceedings IEEE Vehicular Technology Conference (VTC 2008-Fall)*, Calgary, Canada, Sept. 2008; 1–5.
14. Baxley RJ, Zhou GT. Comparison of selected mapping and partial transmit sequence for crest factor reduction in OFDM. In *Proceedings 2006 IEEE Military Communication Conference (MILCOM 2006)*, Washington D.C., USA, October 2006; 1–4.
15. Slimane S. Reducing the peak-to-average power ratio of OFDM signals through precoding. *IEEE Transactions on Vehicular Technology* 2007; **56**(2): 686–695.
16. Wulich D, Goldfield L. Bound of the distribution of instantaneous power in single carrier modulation. *IEEE Transactions on Wireless Communications* 2005; **4**(4): 1773–1778.
17. Ohkubo N, Ohtsuki T. Design criteria for phase sequences in selected mapping. *IEICE Transactions Communications* 2003; **E86-B**(9): 2628–2636.
18. Zhou GT, Peng L. Optimality condition for selected mapping in OFDM. *IEEE Transactions Signal Processing* 2006; **54**(8): 3159–3165.
19. Takei Y, Ohtsuki T. Uplink pre-equalization using mmse prediction for TDD/MC-CDMA systems. In *Proceedings IEEE International Symposium on Personal Indoor and Mobile Radio Communications (PIMRC 2005)*, Berlin, Gremany, Sept. 2013; 291-295.
20. Kawamura T, Kishiyama Y, Sawahashi M. Performance of star 16QAM schemes considering cubic metric for uplink DFT-Precoded OFDMA. *IEICE Transactions on Communications* 2014; **E97-A**: 18–29.
21. Prasad R. *OFDM for Wireless Communication Systems*. Artech House: Massachusetts, 2004.
22. Hassan ES, El-Khamy SE, Dessouky MI‘-, El-Dolil SA, Abd El-Samie FE. Peak-to-average power ratio reduction in space-time block coded multi-input multi-output orthogonal frequency division multiplexing systems using a small overhead selective mapping scheme. *IET Communication* 2008; **3**(10): 1667–1674.
23. Eom SS, Nam HW, Ko YC. Low-complexity PAPR reduction scheme without side information for OFDM systems. *IEEE Transactions Signal Processing* 2012; **60**(7): 3657–3669.
24. Fukuda K, Nakajima A, Adachi F. LDPC-coded HARQ throughput performance of MC-CDMA using ICI cancellation. In *Proceedings IEEE Vehicular Technology Conference (VTC 2007-Fall)*, Baltimore, USA, Sept. 2007; 965–969.
25. Tenma K, Yamamoto T, Lee K, Adachi F. 2-step QRM-MLBD for broadband single-carrier transmission. *IEICE Transaction Communication* 2012; **E95-B** (4): 1366–1374.

AUTHORS' BIOGRAPHIES

Amnart Boonkajay received his BE degree (1st-class honor) in Telecommunications Engineering from Sirindhorn International Institute of Technology (SIIT), Thammasat University, Thailand in 2010, and ME and PhD degrees in Communications Engineering from Tohoku University, Japan in 2013 and 2016, respectively. He is currently working as a government-industry-academia collaboration researcher at Research Organization of Electrical Communication, Tohoku University, where he is doing a research and development for implementing the fifth-generation mobile communication systems. His research interests are based on wireless and mobile communications physical layer including transmit and receive signal processing, filtering and equalization, coding and modulation. He was the recipient of the Japanese Government (MEXT) Scholarship from 2010 to 2016 and the Tohoku University, Department of Electrical and Information Engineering Excellent Student Award in 2016. He is also an active reviewer of technical journals and conference papers and received the IEEE Wireless Communications Letters Exemplary Reviewer in 2015.

Fumiyuki Adachi received his BS and Dr Engineering degrees in Electrical Engineering from Tohoku University, Sendai, Japan, in 1973 and 1984, respectively. In April 1973, he joined the Electrical Communications Laboratories of Nippon Telegraph & Telephone Corporation (now NTT) and conducted various types of research related to digitalcellular mobile communications. From July 1992 to December 1999, he was with NTT Mobile Communications Network, Inc. (now NTT DoCoMo, Inc.), where he led a research group on wideband/broadband CDMA wireless access for IMT-2000 and beyond. He contributed to the development of 3G air interface standard, known as W-CDMA. Since January 2000, he has been with Tohoku University, Sendai, Japan. He was a full Professor until March 2016 and is now a specially appointed Professor for research. His research interest is in the area of wireless signal processing and networking including broadband wireless access, equalization, transmit/receive antenna diversity, MIMO, adaptive transmission, and channel coding. He was a program leader of the 5-year Global COE Program 'Center of Education and Research for Information Electronics Systems' (2007-2011), awarded by the Ministry of Education, Culture, Sports, Science and Technology of Japan. From October 1984 to September 1985, he was a United Kingdom SERC Visiting Research Fellow in the Department of Electrical Engineering and Electronics at Liverpool University. He is an IEICE Fellow and is a Co-recipient of the IEICE Transactions best paper of the year award 1996, 1998, and 2009 and also a recipient of Achievement award 2003. He is an IEEE Fellow and is a VTS Distinguished Lecturer since 2011. He is a Co-recipient of the IEEE Vehicular Technology Transactions best paper of the year award 1980 and again 1990 and also a Recipient of IEEE VTS Avant Garde award 2000. He is a Recipient of Thomson Scientific Research Front Award 2004, Ericsson Telecommunications Award 2008, Telecom System Technology Award 2009, Prime Minister Invention Prize 2010, British Royal Academy of Engineering Distinguished Visiting Fellowship 2011, KDDI Foundation Research Award 2012, IEEE VTS Conference Chair Award 2014, C&C Prize 2014, and Rinzaburo Shida Award 2016. He is listed in Highly Cited Researchers 2001 (http://highlycited.com/archives/).